4522 *Chem. Mater.* **2010,** *22,* 4522–4524
DOI:10.1021/cm101254j

CHEMISTRY OF MATERIALS
Communication

Exfoliated MoS_2 Nanocomposite as an Anode Material for Lithium Ion Batteries

Jie Xiao, Daiwon Choi, Lelia Cosimbescu, Phillip Koech, Jun Liu, and John P. Lemmon*

Pacific Northwest National Laboratory, Richland, Washington 99354

Received May 4, 2010
Revised Manuscript Received July 16, 2010

Conventional Li-ion batteries utilize graphite as the anode materials. The low theoretical capacity of graphite (372 mA h/g) makes it important to find alternative negative electrodes. Si (4200 mA h/g)[1] or Sn (994 mA h/g)[2] attract much interest because of their high capacity. The application of Si or Sn anodes in lithium ion batteries has been limited by their poor cycling characteristic caused by large volume changes which occur during the repeated alloying and dealloying process with lithium. Recent reports show that the pulverization problem associated with Si or Sn can be successfully resolved by the control of particle morphology[3] and appropriate selecting of good conductive additives[4] and binders.[5] Another promising material MoS_2 with unique properties has attracted interest in several applications including hydrogen storage,[6] as catalysts,[7] lubricants,[8] and double-layer capacitor.[9] The weak van der Waals interaction between MoS_2 layers allows Li^+ ions to diffuse without a significant increase in volume expansion. Because of these properties, MoS_2 was intensively studied as a cathode[10] material in the early development of lithium ion batteries. The investigation of MoS_2 as an anode material for Li-ion batteries has also been reported[11−13] and the particle size and morphology was shown to have significant influence on the electrochemical properties of the disordered MoS_2. The authors suggest the large increase in the observed lithium capacity is mainly due to voids and dislocations in the disordered MoS_2. Lemmon et al.[14,15] previously reported that single-phase MoS_2/PEO nanocomposite can be prepared by the hydrolysis of lithiated MoS_2. However, the electrochemical properties of the as-prepared materials were not investigated. It was suggested that nanocomposites may provide improved performance by inserting the lithium ion coordination properties of PEO into the interlayer spacing of MoS_2 allowing for increased ion transfer. This property along with the reported increase of capacity in restacked MoS_2[11] has led us to revisit this material as an anode for Li-ion batteries. Significant improvements of reversible capacity is reported in this work.

Figure 1 compares the XRD patterns of nanocomposites comprised of exfoliated MoS_2 with various amounts of PEO where the overall stoichiometry is $Li_{0.12}(PEO)_yMoS_2$ ($y < 1$). A broad peak at 5−7° appears only after PEO addition and corresponds to the (001) reflection of a highly disordered MoS_2/PEO composite. The reflection is equivalent to an ~8 Å increase in the MoS_2 interlayer spacing and indicates the addition of PEO in the MoS_2 gallery when the PEO loading ratio is increased from 0.05 to 0.15. The slight increase in intensity observed with increasing amounts of PEO in the nanocomposite suggests a more ordered phase and is consistent with previous reports.[15,16] The large broad peak present at 12−14° represents a possible combination of the nanocomposite (002) reflection, and restacked or unexfoliated MoS_2 (002) after exfoliation (See Figure 2b).

The HRTEM images for PEO/MoS_2 = 0.05 composite are shown in Figure 2. After exfoliation the randomly stacked MoS_2 sheets is clearly visible with an expanded *d*-spacing consistent with the XRD pattern. However, the micrographs show MoS_2 coexists with the nanocomposite, as shown in Figure 2b, where the ordered *d*-spacing matches that of the pristine or restacked MoS_2. This observation confirms our explanation for the combined (002) peaks in Figure 1, suggesting that it is possible to further improve the capacity of the composite by further optimizing the synthesis condition.

The morphologies of the original lithiated MoS_2, exfoliated MoS_2 and PEO/MoS_2 composite are compared in Figure 3. The micrometer-sized original MoS_2 (Figure.3a) consists of small platelike particles which are distributed randomly. After exfoliation, the morphology of MoS_2 in Figure.3b interestingly changes to sandwichlike secondary particles with a thickness of 10 μm. With the addition of PEO during exfoliation (Figure.3c), the layered morphology

*Corresponding author. E-mail: John.Lemmon@pnl.gov Pacific Northwest National Laboratory, K2-03, P.O. Box 999, Richland, WA 99352. Tel: (509) 375-6967. Fax: (509) 375-4448.

(1) Wilson, A. M.; Way, B. M.; Dahn, J. R. *J. Appl. Phys.* **1995**, *77*, 363.
(2) Yua, Y.; Gub, L.; Dhanabalana, A.; Chen, C.; Wang, C. *Electrochim. Acta* **2009**, *54*, 7227.
(3) Lee, J. K.; Smith, K. B.; Hayner, C. M.; Kung, H. H. *Chem. Commun.* **2010**, *46*, 2025.
(4) Liu, W.; Guo, Z.; Yung, W.; Shieh, D.; Wu, H.; Yang, M.; Wu, N. *J. Power Sources* **2005**, *140*, 139.
(5) Liu, G. *Annual Merit Review, Batteries for Advanced Transportation Technology Program*; U.S. Department of Energy: Washington, D.C., June, 2010.
(6) Chen, J.; Kuriyama, N.; Yuan, H. T.; Takeshita, H. T.; Sakai, A. *J. Am. Chem. Soc.* **2001**, *123*, 11813.
(7) Sun, M. Y.; Adjaye, J.; Nelson, A. E. *Appl. Catal., A* **2004**, *263*, 131.
(8) Chhowalla, M.; Amaratunga, G. A. *Nature* **2000**, *407*, 164.
(9) Soon, J. M.; Loh, K. P. *Electrochem. Solid-State Lett.* **2007**, *10*, A250.
(10) Murugan, A. V.; Quintin, M.; Delville, M. H.; Campet, G.; Gopinath, C. S.; Vijayamohanan, V. *J. Power Sources* **2006**, *156*, 615.
(11) Feng, C.; Ma, J.; Li, H.; Zeng, R.; Guo, Z.; Liu, H. *Mater. Res. Bull.* **2009**, *44*, 1811.
(12) Whittingham, M. S. *Science* **1976**, *192*, 1126–1127.
(13) Johnson, C. S.; Li, N.; Lefief, C.; Thackeray, M. M. *Electrochem. Commun.* **2007**, *9*, 787.
(14) Murphy, D. W.; DiSalvo, F. J.; Hull, G. W.; Waszczak, J. V. *Inorg. Chem.* **1976**, *15*, 17.
(15) Lemmon, J. P.; Lerner, M. M. *Chem. Mater.* **1994**, *6*, 207.
(16) Harris, D. J.; Bonagamba, T. J.; S-Rohr, K. *Macromolecules* **1999**, *32*, 6718.

 Published on Web 07/30/2010

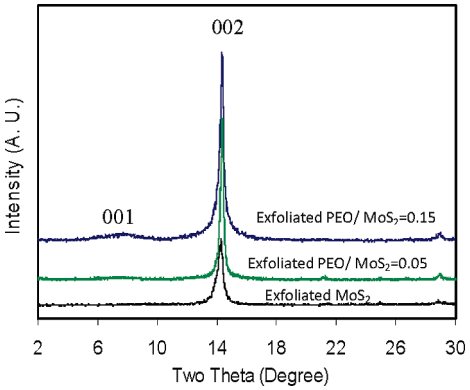

Figure 1. XRD comparison of the exfoliated MoS_2 with different amounts of PEO.

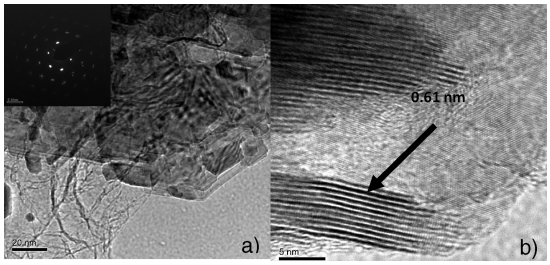

Figure 2. TEM images for exfoliated PEO/MoS_2 = 0.05 composite. (a) MoS_2 sheets with expanded spacing after the incorporation of PEO. (b) Restacked MoS_2 without PEO intercalation is also observed in the composite.

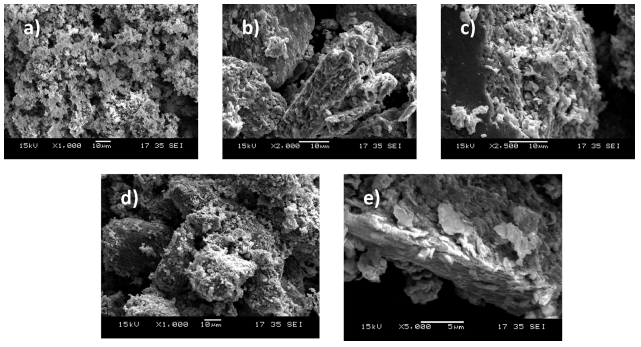

Figure 3. SEM images of (a) original lithiated MoS_2, (b) exfoliated MoS_2, and PEO/MoS_2 composite with different reaction stoichiometries: (c) PEO/MoS_2 = 0.05, (d)PEO/MoS_2 = 0.15, and (e) PEO/MoS_2 = 0.15 with enlarged image.

of MoS_2/PEO composite becomes more pronounced. Each of the layers in Figure 3c is composed of the small plate-shape particles from Figure 3a. The restacking of these layers forms the secondary particles with some of the small platelike particles reside in between the layers. Increasing the weight ratio of PEO/MoS_2 to 0.15 during exfoliation further improves the layered character of the composite (Figure. 3d, e) with a reduced amount of smaller individual particles. The large micrometer-sized secondary particles of the MoS_2/PEO nanocomposite were observed to have a practical tap density that is beneficial to facilitating the manufacturing of commercial cells. Additionally, the distance of pores between each single layer in the secondary particle ensure the flooding of the electrolyte and can increase the utilization rate of the micrometer-sized materials.

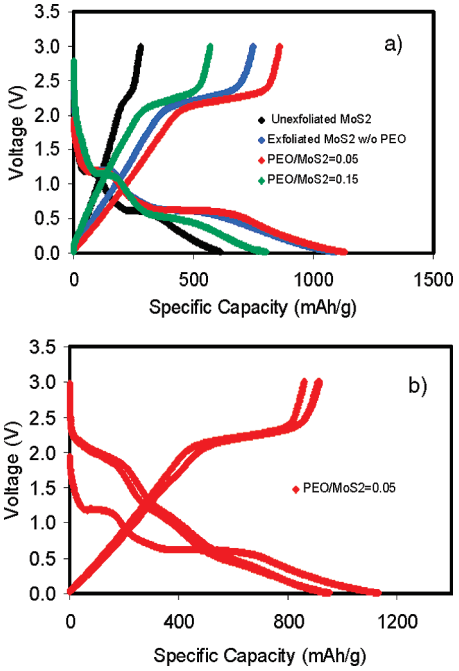

Figure 4. (a) Comparison of the first charge−discharge curves for unexfoliated MoS_2 and exfoliated MoS_2 with different amounts of PEO. (b) Subsequent charge−discharge curves of PEO/MoS_2 = 0.05 composite.

The first charge−discharge curves of the original MoS_2 and exfoliated MoS_2 with different amounts of PEO are compared in Figure 4a. In the first discharge (Li insertion) three plateaus at ~1.1, 0.8, and 0.6 V are observed for all the MoS_2 electrodes. The first plateau at 1.1 V is indicative to the formation of Li_xMoS_2 and earlier reports[17,18] by other groups attribute the plateau variation to the lithium intercalation on different defect sites of MoS_2. However, that mechanism does not explain the absence of the 2.2 V discharge plateau in the first lithiation cycle or the charge balance necessary to maintain with the increase in lithium capacity. The plateaus at 1.1 and 0.6 V disappear in the first charge (Li extraction), whereas another new plateau at ~2.2 V evolves and is reversible in the subsequent cycles (see Figure 4b). The 0.6 V plateau should be related to the reduction of Mo^{4+} to Mo metal accompanied by the formation Li_2S. This mechanism also explains the formation of 2.2 V reversible redox plateaus in the following cycles. We are now utilizing in situ XRD characterization to further confirm this explanation.

Theoretically the capacity of MoS_2 is only 167 mA h/g if only one mole of Li^+ is intercalated. However, the first discharge capacity of the pristine MoS_2 is slightly above 600 mA h/g with a fast decrease to 200 mA h/g (Figure 5) in the second cycle suggesting either poor reversibility of Li^+ in the pristine MoS_2 or the irreversibility of the Mo redox couple. Most of the Li^+ ions are trapped in the unexfoliated structure after the first discharge.

Because of the increased structural disorder in the exfoliated MoS_2, more Li^+ ions can reversibly interact with

(17) Dominko, R.; Arcon, D.; Mrzel, A.; Zorko, A.; Cevc, P.; Venturini, P.; Gaberscek, M.; Remskar, M.; Mihailovic, D. *Adv. Mater.* **2002**, *14*, 1531.
(18) Wang, G. X.; Bewlay, S.; Yao, J.; Liu, H. K.; Dou, S. K. *Electrochem. Solid-State Lett.* **2004**, *7*, A321.

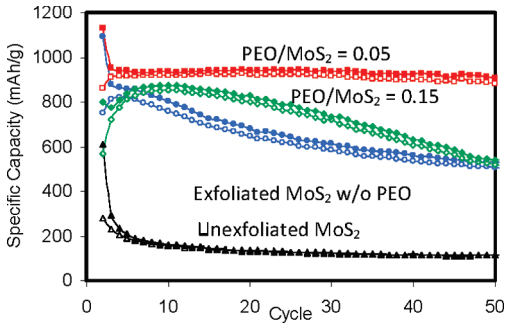

Figure 5. Comparison of cycling stability for unexfoliated MoS_2 and exfoliated MoS2 with different amounts of PEO. All cells were cycled between 0.01 and 3.0 V at 50 mA/g. Solid symbols, Li insertion; open symbols, Li extaction.

the expanded MoS_2 structure. Accordingly, the initial discharge capacity increases to above 1000 mAh/g and indicates much of the capacity gain is derived from the accessibility of Li^+ to form Li_2S and Mo metal. Although the reversible capacity gradually decays for the exfoliated MoS_2 the discharge capacity is maintained above 500 mA h/g after 50 cycles and is much higher than that of the pristine MoS_2.

Interestingly, when a small amount of PEO (PEO/MoS_2 = 0.05) is added during the exfoliation process, not only does the initial capacity double from that of the pristine MoS_2 but the capacity retention is significantly improved, as shown in Figure 5. Considering the fact that the capacity for the PEO/MoS_2 composite is calculated from the total weight of the MoS_2 and PEO (5 wt % PEO), the specific capacity of MoS_2 in the composite should be slightly higher than 1131 mA h/g. The irreversible capacity loss for PEO/MoS_2 = 0.05 composite is 178 mA h/g and may be due to the unexfoliated MoS_2 or restacked MoS_2 in the composite as shown in the TEM. Electrolyte decomposition should also partially contribute to the irreversible capacity. The Coulombic efficiency is maintained above 95% from the second cycle suggesting a high reversibility reaction with Li^+ ions.

The results show the incorporation of PEO plays a key role in increased performances observed for the PEO/MoS_2 nanocomposites. The findings indicate that PEO absorbed on the MoS_2 sheets can stabilizes the disordered structure throughout the cycling regime to accommodate more Li^+ ions. The ionic conductivity is facilitated by any remaining Li-doped PEO, which directly coats the larger MoS_2 particle surface. Because Li-doped PEO[19] is widely used as the polymer electrolyte in Li-ion batteries, it is possible for the coated PEO to accelerate the Li^+ transportation between the solid particle and electrolyte.[20] Further increasing the PEO amount from 0.05 to 0.15 lowers the capacity and cyclability of the composite. Previous results showed that increasing the PEO ratio can lead to highly order nanocomposites.[15,16] This suggests the increased cystallinity accompanying the more order nanocomposites may lead to decrease lithium accessibility. The increased amounts of PEO may also decrease the electronic conductivity resulting in higher internal resistance and charge transfer. Although the charge cutoff voltage is relatively high for anode application, it is tunable by optimizing the cutoff voltage in combination with a high voltage cathode material. Most importantly, the utilization of PEO polymer provides an effective approach to significantly improve the performance of MoS_2 anode and can be applied to many other materials with similar structures.

Lithiated MoS_2 was prepared according to the earlier literature method.[11] Poly-(ethylene oxide) (PEO, Aldrich, M_w = 600 000) was used as-received. The preparation of nanocomposite proceeds by exfoliation of the layered disulfide[12] to form a colloid followed by the adsorption of the PEO polymer into these separated lamella. Exfoliation of MoS_2 into single sheets was achieved through the rapid hydrolysis and sonication of Li_xMoS_2. 10 mg PEO was dissolved in 20 mL of D.I. water first and then poured into the Li_xMoS_2 quickly and keep sonication for 2 h. This dispersion was then separated by centrifugation. Without washing the nanocomposite was dried at 80 °C overnight. The weight ratio of PEO/Li_xMoS_2 is 5 or 15%. As a control the exfoliated MoS_2 without any PEO was also prepared. The crystalline structures of the MoS_2/PEO composites were determined by X-ray diffraction (XRD) using a Philips Xpert X-ray diffractometer in θ-2θ scan mode and a CuKα tube (λ = 1.54178 Å) at 0.5° min^{-1}. A JEOL 5900 SEM (scanning electron microscope) equipped with a Robinson Series 8.6 BSE (backscattered electron) detector, and an EDAX Genesis EDS (energy-dispersive spectroscopy) system with a Si (Li) EDS detector was used to investigate the particle morphology. Electrodes were prepared by casting a slurry of the MoS_2/PEO composite, super P (from Timcal), and poly(vinylidene fluoride) (PVDF, KYNAR HSV900 from Arkema Inc.) in *N*-methyl pyrrolidone (NMP from Aldrich) solvent onto a copper foil (Pred. Materials International, Inc.). After drying, the electrodes were punched into 1.4 cm ø disks. The typical loading of the active materials in the electrode is 1−5 mg/cm^2. Lithium metal was used as an anode in a type 2325 coin-cell (CNRC, Canada) system assembled in an argon-filled glovebox (MBraun Inc.). The electrolyte consisted of 1 M $LiPF_6$ in a mixture of ethylene methyl carbonate (EMC) and ethylene carbonate (EC) at a 7:3 volume ratio. The electrochemical tests were performed on an Arbin BT-2000 Battery Tester at room temperature. The cells were cycled between 0.01 and 3.0 V vs Li/Li^+ at 50 mA/g unless otherwise specified.

Acknowledgment. The authors gratefully acknowledge financial support from PNNL's internal DOE-LDRD funding and extend their gratitude to Professor Michael Lerner at Oregon State University for insightful comments and discussion.

(19) Liu, G.; Reinhout, M. T.; Baker, G. L. *Solid State Ionics* **2004**, *175*, 721.
(20) Kang, B.; Ceder, G. *Nature* **2009**, *458*, 190.